A Prospective Multimodal Imaging Assessment of Cervical Lymphadenopathy: Evaluating the Incremental Diagnostic Performance of B-mode Ultrasonography and Elastography with Histopathological Correlation in the Differentiation of Benign and Malignant Etiologies

Makarand Wadibhasme[1*], Chaithanya Isamalla[2], Madireddy Veena[3], Sarika Bolenwar[4] and Shirisha Jakka[5]

[1]Consultant Radiologist, CIIMS Hospital, Nagpur, Maharashtra, India
[2]Senior Consultant Radiologist, AIG Hospitals, Hyderabad, Telangana, India
[3]Professor of Radiodiagnosis, Government Medical College, Sangareddy, Telangana, India
[4]Consultant Radiologist, Vijaya Diagnostic Centre, Hyderabad, Telangana, India
[5]Senior Consultant Radiologist, Head of Women's Imaging, Krishna Institute of Medical Sciences (KIMS) Hospital, Hyderabad, Telangana, India

Abstract

The aim of the study is to evaluate the role and diagnostic utility of B-mode ultrasonogram and elastography prospectively to differentiate the benign and malignant causes of cervical lymphadenopathy and the primary objective is to compare the results of ultrasonogram and elastography with histopathological examination (HPE) in order to determine the accuracy and efficacy of sonoelastography in differentiating: benign nodes (including reactive and tuberculous lymphadenitis) from malignant nodes (metastatic carcinoma and lymphoma) and among benign nodes, distinguishing tuberculous from reactive lymphadenitis where possible. Whereas the secondary objectives are to: a) determine the individual as well as combined role of ultrasonogram, Doppler and elastography in categorizing the benign and malignant nature of lymph nodes; b) to determine the role of sonoelastography in staging of head and neck cancers with cervical lymphadenopathy; and c) to evaluate replacing invasive methods like fine needle aspiration cytology (FNAC)/biopsy with non-invasive elastography for diagnosing malignant nodes.

Keywords: Cervical lymphadenopathy, B-mode Ultrasonography, Elastography, Etiologies

Introduction

Cervical lymphadenopathy is a prevalent clinical condition in the human body, affecting around 300 lymph nodes in the head and neck region. The condition can be caused by infection, inflammation, or malignant conditions. In children, it is primarily due to infection, with viral, bacterial, or protozoal agents contributing to the development of reactive hyperplasia [1].

Tuberculosis (TB) is a significant contributor to infectious diseases, with India having the highest prevalence of this disease. Lymphadenitis, an extrapulmonary manifestation of TB, is more common in cervical lymph nodes, constituting approximately 63% of cases. The demographic most affected by this phenomenon is children and young adults aged 11 - 30, with a slight preference towards females. Human

immunodeficiency virus is another etiological factor contributing to the development of lymphadenopathy, with extra-pulmonary nodal TB being a prevalent manifestation in affected individuals [2].

Malignancy incidence is higher in adults compared to children, with secondary metastases often arising from malignancies originating in the head and neck region. Primary lymphadenopathy is the most frequently encountered form of lymphoma. Cervical lymphadenopathy can sometimes manifest as the initial symptom or indication of disease in instances of metastasis [3].

While the present study aims to differentiate benign from malignant cervical lymphadenopathy, it is important to note that in regions with high TB prevalence such as India, tuberculous lymphadenitis-though benign in nature-may exhibit imaging and elastographic features

that overlap with malignancy. Therefore, special attention is given to distinguishing tuberculous nodes from neoplastic nodes in the analytical framework [4].

In regions with a high prevalence of TB, such as India, tuberculous lymphadenitis often presents with central caseous necrosis, which can mimic the necrotic appearance of malignant nodes on both B-mode ultrasound and elastography. Consequently, elastographic patterns indicative of necrosis-such as pattern 4-may be observed in both malignant and tuberculous nodes, posing a significant diagnostic challenge and potentially reducing the specificity of elastography in such settings [5].

The presence of cervical lymphadenopathy plays a pivotal role in the staging, treatment, and prognosis of the condition. Patients with ipsilateral cervical lymphadenopathy experience a decrease in their 5-year survival rate to 50%, bilateral cervical lymphadenopathy is associated with a decreased 5-year survival rate of 25%, and extra capsular extension of nodal metastasis results in a further 50% reduction. Assessment of these nodes is crucial for patient prognosis evaluation and treatment planning [6].

Classification

In 1938, Rouviere [7] classified cervical nodes into two groups: the anterior and posterolateral groups, and another cluster encircling the upper respiratory and digestive tract. The researchers accurately delineated the anatomical positioning of the nodes and charted their respective drainage regions. However, surgeons' lack of familiarity with anatomically based terminologies for neck node dissection led to a shift in the trajectory of nodal classification [8].

In 1981, Shah et al. [9] proposed a simplified numerical classification system utilizing levels for the identification of nodes, drawing upon clinical and pathophysiological information. The facial, parotid, mastoid, occipital, and retropharyngeal nodes were excluded from the neck dissection framework (Table 1).

Imaging

B-mode ultrasonography is the primary diagnostic method for cervical lymphadenopathy, with a heightened sensitivity of 73% when combined with Doppler analysis. This technique is non-invasive, rapid, and cost-effective, demonstrating superior performance in detecting small lymph nodes measuring less than 5.5 millimeters (mm). The criteria used in B-mode ultrasound include size, shape, borders, presence or absence of the hilum, ratio of the cortex to hilum, echogenicity, and homogeneity of internal structures [10].

Typical lymph nodes have an oval shape with a hypoechoic cortex and an echogenic hilus. Reactive lymph nodes exhibit similar characteristics to normal nodes on grey scale sonography. Tuberculous lymph nodes are round, hypoechoic, and matted with a loss of echogenic hilus due to intranodal cystic necrosis. Metastatic nodes are hypoechoic, rounded structures lacking echogenic hilus and displaying varying degrees of necrosis. Cystic necrosis is a frequently observed phenomenon that indicates the malignant nature of nodules, particularly in cases of metastasis associated with squamous cell carcinoma [11].

Color Doppler sonography has proven highly accurate in differentiating between benign and malignant cervical nodes, with a high accuracy rate ranging from 83% to 89% for sensitivity and 76% to 98% for specificity. Both normal and reactive lymph nodes can exhibit hilar vascularity or apparent avascularity. Malignant lymph nodes demonstrate either peripheral or mixed hilar and peripheral vascularity, closely linked to tumor neoangiogenesis and the recruitment of capsular vessels. Tuberculous nodes exhibit a vascular pattern that resembles both benign and malignant nodes, with the displacement of hilar vessels associated with focal necrotic regions distinguishing them from the normal category [12].

Despite multiple proposed criteria for distinguishing between benign and malignant nodes, there is ongoing debate regarding the most specific or noteworthy feature. The current detection method lacks the ability to identify micro metastasis in lymph nodes, potentially leading to false negative outcomes. Therefore, it is crucial to emphasize pathological diagnosis for accurate assessment [13].

Elastography

Elastography is a noninvasive imaging technique that uses the elasticity of tissue to distinguish between benign and malignant lesions. It is based on the principle of Young modulus, which is a biomechanical parameter that indicates the degree of hardness in tissue. The technique has gained popularity due to its cost-effectiveness, technical simplicity, and accessibility [14].

Manual palpation relies on qualitative estimation of the tissue's Young modulus (E), which is defined as σ/ϵ, external compression (stress) and tissue deformation due to compression (strain). However, advancements in imaging technology have improved the ability to generate a comprehensive and precise representation of tissue stiffness, revitalizing the palpatory approach [15].

Sonographic elastography uses a conventional sonography machine with special software and an ultrasound probe. A mechanical force is delivered to the biological tissue, and echo data before and after the force is obtained. Digital measurements of tissue hardness are performed, and a map of soft-tissue deformation is created. The resultant image is called a sonoelastic image or elastogram, which is color coded [16].

Table 1: Simplified numerical classification system.

Level	Location
IA	Submental lymph nodes
IB	Submandibular lymph nodes
II	Internal jugular (deep cervical) chain from the base of the skull to inferior border of the hyoid bone
III	Internal jugular (deep cervical) chain from the hyoid bone to the inferior border of the cricoid arch
IV	Internal jugular (deep cervical) chain between the inferior border of the cricoid arch and the supraclavicular fossa
VA	Posterior triangle or spinal accessory nodes from base of skull to the inferior border of the cricoid arch
VB	Posterior triangle or spinal accessory nodes from the inferior border of the cricoid cartilage to the clavicle
VI	Central compartment nodes from the hyoid bone to the suprasternal notch
VII	Nodes inferior to the suprasternal notch in the upper mediastinum

The compressibility of tissue, also known as strain, represents the variation in tissue displacement relative to its distance from the probe. Elastography has been applied to various anatomical structures, such as breast, liver, thyroid, cervical nodes, prostate, cervix, and blood vessels [17].

Initially applied to the breast in 1997, it has since been applied to the liver, thyroid, and cervical lymph nodes. Recent advancements in this field include early detection and differential diagnosis of focal diseases, improved accuracy for diagnosing diffuse diseases, and assessment of response to treatments. Sonoelastography can demonstrate the stiffness of both the cortex and medulla of lymph nodes and detect early circumscribed malignant infiltration [18].

Sonoelastography allows visualization of tissue stiffness through color mapping or Shear wave velocity. The fundamental concept underlying sonoelastography is based on tissue reactions, such as changes in displacement, strain, or speed, by applying an external or internal static or dynamic excitation [19].

Strain elastography

Strain elastography is an innovative sonoelastographic technique that measures tissue strain or displacement during mechanical excitation, providing a noninvasive estimation of tissue stiffness or elasticity. It is widely supported by radiologists due to its technical ease, efficiency, and compatibility with routine ultrasonographic examinations [20]. The technique allows for dynamic examination of lesions during compression, which occur in the longitudinal direction or axis of the beam or applied force, known as bulk or compression waves.

External compression is a commonly employed technique, consisting of alternating cycles of compression and decompression. The application of compression should be gentle, light, and consistent, with the suppression of lateral hand movement [21]. High-speed algorithms are used to estimate real-time strain distribution, and some machines have a quality factor that informs the examiner about the level of compression and provides feedback on its quality.

Internal compression is infrequently employed, relying on inherent stresses such as arterial pulsations, cardiovascular movements, or other physiological motions to displace the tissue. This approach has limitations, such as the lack of proximity between the lesions or nodes and the carotid artery or other pulsating structures [22].

B-mode images of the specified region are acquired, followed by the elastography mode activated, and the process is conducted according to the aforementioned explanation. The data obtained is visually represented as a two-dimensional map illustrating the relative strain of the tissue, commonly referred to as an elastogram [23-26].

A four-point rating scale was employed in a grey scale elastography study to assess qualitative criteria including lymph node visibility, relative brightness, margin regularity, and margin definition. Color-coded images are assigned one of 256 distinct colors based on the level of strain exhibited by the corresponding tissue, with blue representing soft tissue experiencing the highest level of strain, green representing an average level of strain, and red representing hard tissue experiencing the least amount of strain (Table 2).

Compression-based strain elastography has evolved from qualitative interpretations to semi-quantitative results using the strain index or strain ratio. Two regions of interest (ROI) and a reference region are used to calculate the average stiffness of the two areas. The ratio between ROI of the comparable portion and ROI of the lesion determines the relative stiffness of the lesion. Consistency in the size of the ROI is crucial for accuracy. A strain ratio exceeding 1.5 indicates reduced strain, increased stiffness, and higher acceptability rates. An upward trend indicates an increased likelihood of malignancy [28].

Shear wave elastography

This particular elastography modality is not acquired through manual compression. The technique employs an acoustic radiation force impulse (ARFI) in the form of an ultrasound-generated push pulse to induce displacement of the tissue beneath. The visual representation produced through ARFI imaging is commonly referred to as an elastogram. The visual representation can be categorized into color-coded or black and white formats, contingent upon the specific manufacturer's choice [29]. The dimensions and shape of the lesions observed on an elastogram are contingent upon the level of stiffness exhibited by the lesions. Stiff nodules exhibit increased size when visualized on an elastogram.

Literature Review

Researchers have explored the potential of strain and shear wave elastography in distinguishing between benign and malignant cervical lymphadenopathy. The term "elastography" has evolved into a comprehensive designation encompassing various techniques for imaging elasticity. In 2007, Lyshchik et al. [30] conducted a clinical prospective study to assess the diagnostic efficacy and accuracy of strain elastography in distinguishing between benign and malignant cervical lymph nodes. The study involved 141 lymph nodes; 43 patients diagnosed with suspected thyroid and hypopharyngeal carcinoma exhibiting nodal metastasis. The nodes were classified according to their visual appearance, relative brightness compared to neighboring muscles, and the regularity of the outline and margin definition.

In 2008, Alam et al. [27] conducted a prospective study involving 85 lymph nodes obtained from 37 consecutive patients. The individual employed a 5-point elastographic pattern that relied on the quantification of high and low elastic regions within the node. The cumulative scores of these five criteria were assessed using a threshold of 6/7 to distinguish between reactive and malignant lymph nodes. The study reported a sensitivity of 98%, specificity of 59%, and accuracy of

Table 2: Patterns and scoring system on elastographic findings (Quoted from Alam et al. [27]).

Pattern	Description	Elastographic diagnosis
1	Absent or very small red area(s)	Benign
2	Small scattered red areas, total red area <45%	Benign (Reactive)
3	Large red area(s), total red area ≥45%	Malignant
4	Peripheral red area and central green area, suggesting central necrosis	Malignant
5	Red area with or without a green rim	Malignant

Note: Here red represents hard area and blue represents soft area. Intermediate is green.

84% for grey scale ultrasound. The sensitivity, specificity, and accuracy values for elastography were determined to be 83%, 100%, and 89% respectively. In the case of the combined evaluation of ultrasound and elastography, these values were found to be 92%, 94%, and 93% respectively.

In 2009, Rubaltelli et al. [31] conducted a study involving 53 patients with cervical lymphadenopathy, using ultrasonography and sonoelastography to assess the condition. The results indicated a sensitivity of 75%, specificity of 80%, accuracy of 77%, positive predictive value (PPV) of 80%, and negative predictive value (NPV) of 70%. Zhang et al. [32] conducted a retrospective study on cervical lymph nodes, examining 155 cervical lymph nodes using B-mode ultrasound, power Doppler ultrasonography, and sonoelastography techniques. The sensitivity and specificity values for elastography were determined to be 78.41% and 98.51%, with the Youden index attained its maximum value at this threshold.

In 2010, Bhatia et al. [33] conducted a study on 74 cervical nodes, determining 37 benign and 37 malignant using real-time qualitative sonoelastography. The study used a retrospective design and FNAC after elastography. The elastographic patterns were assessed by three independent observers, with the median score for benign nodes being 2, and for malignant nodes being 3. The results suggest that real-time sonoelastography needs enhancements to be widely accepted as a standard diagnostic procedure.

Tan et al. [34] conducted a retrospective study on cervical lymph nodes, analyzing 128 lymph nodes using ultrasound, power Doppler, and elastography. The strain ratio was calculated, and the results showed that a strain ratio exceeding the specified threshold exhibited considerable usefulness. The inter-observer agreement demonstrated a higher kappa value, suggesting that elastography has the potential to serve as an adjunctive tool for evaluating and distinguishing between benign and malignant cervical nodes.

Ishibashi et al. [35] conducted a retrospective study involving 19 patients with squamous cell carcinoma of the oral cavity, comparing the utility of B-mode ultrasound, power Doppler, and elastography. They found that both conventional ultrasound and elastography yielded sensitivity, specificity, and accuracy rates of 90.3%, 80%, and 84.5%, respectively. Teng et al. [36] evaluated the effectiveness of elastography, in conjunction with B-mode ultrasound and power Doppler, in distinguishing between benign and malignant cervical lymph nodes.

Lenghel et al. [37] introduced a novel scoring system consisting of eight patterns and assessed its diagnostic efficacy. The receiver operating characteristic (ROC) curve yielded an area of 0.846, indicating a reasonably accurate discrimination between benign and malignant cases. The proposed scoring system exhibited high levels of inter-observer agreement, favorable specificity, and reasonable sensitivity.

In 2013, Lo et al. [38] conducted a retrospective study to evaluate the effectiveness of real-time elastography in detecting malignant lymph nodes in cases of enlarged cervical lymph nodes. The study involved 131 patients who underwent ultrasonography, elastography, and FNAC. The researchers used a four-point visual scale for elastography and developed an expanded model incorporating four preceding predictors and an elasticity score through a logistic regression model. The histopathological findings showed that 77 lymph nodes were benign, while 54 were identified as malignant. The elasticity score system

demonstrated sensitivity and specificity rates of 66.7% and 57.1%, respectively. The PPV and NPV were 52.2% and 71.0%, respectively. The prediction model system exhibited sensitivity, specificity, PPV, and NPV of 79.6%, 92.2%, 87.8%, and 86.6%, respectively.

In 2014, Fu et al. [39] conducted a retrospective study involving 39 patients with unexplained cervical lymphadenopathy. They assessed the clinical significance of real-time elastography using a quantitative approach, using grey scale ultrasound, power Doppler, and real-time sonoelastography. The results revealed notable distinctions between the groups in terms of elastography, with 9 patients successfully diagnosed with definitive outcomes.

- Early studies primarily utilized qualitative or semi-quantitative strain elastography. Lyshchik et al. [30] prospectively evaluated strain elastography in 141 lymph nodes, using visual appearance and relative brightness to differentiate benign from malignant nodes, reporting promising diagnostic accuracy. Alam et al. [27] introduced a 5-point elastographic pattern system, achieving high sensitivity (83%) and specificity (100%). Subsequent studies by Rubaltelli et al. [31] and Bhatia et al. [33] reinforced the utility of strain elastography, though inter-observer variability and operator dependence were noted as limitations.

- With technological advancements, shear wave elastography and ARFI imaging enabled quantitative stiffness measurements. Studies such as those by Zhang et al. [32] and Teng et al. [36] incorporated strain ratios and shear wave velocity, demonstrating improved objectivity. However, consensus on diagnostic thresholds remained lacking, and applicability in deep cervical nodes was technically challenging.

- Several investigators evaluated elastography as an adjunct to conventional ultrasonography and Doppler. Lo et al. [38] developed a prediction model combining B-mode features with elasticity scores, achieving high specificity (92.2%). A meta-analysis by Fu et al. [39] concluded that real-time strain elastography had high accuracy but emphasized the need for standardization in clinical implementation.

- A notable gap in the existing literature is the limited focus on differentiating tuberculous lymphadenitis from malignancy in high-prevalence regions. Most elastography studies originated from western populations where TB is less common, leading to a lack of diagnostic criteria applicable in endemic settings. The overlapping elastographic patterns between necrotic TB nodes and malignant nodes-a critical diagnostic dilemma-remained underexplored.

Research gap and justification for present study

Despite the growing body of evidence supporting elastography in cervical lymph node assessment, several key issues persist: (1) the majority of studies are retrospective and lack prospective validation in diverse clinical settings; (2) there is insufficient emphasis on differentiating tuberculous from malignant lymphadenopathy in endemic regions; (3) comparative evaluation of the incremental value of elastography over conventional ultrasound and Doppler is limited; and (4) qualitative pattern-based systems dominate, with underutilization of quantitative elastographic parameters.

A meta-analysis of nine studies [40-48] examining the diagnostic value of real-time strain elastography studies found that elastography demonstrated high accuracy in the classification of superficial cervical lymph nodes, potentially aiding in the identification of suspicious lymph nodes and guiding the decision to perform a biopsy. However, further research is needed to comprehensively comprehend the

manifestation of diverse diseases in the context of elastography in the United States and establish uniformity in clinical implementation.

This prospective study was therefore designed to evaluate the diagnostic utility of combined B-mode ultrasonography, Doppler, and strain elastography in a cohort from a TB-endemic region, with explicit focus on differentiating not only benign from malignant nodes but also distinguishing tuberculous lymphadenitis from other benign and malignant causes. Furthermore, we aimed to assess whether elastography provides significant added diagnostic value beyond conventional ultrasound alone.

Materials and Methods

The institutional ethical committee approval was obtained properly before the commencement of the study. Permission was obtained from the department of pathology in a proper way to obtain the histopathological report for correlation. Prospectively all the patients meeting the inclusion criteria during study period are enrolled.

A study was performed at Krishna Institute of Medical Sciences (KIMS), Secunderabad, Telangana, India, in accordance with the guidelines of the ethical committee of the hospital and carried out for a period of 10 months (from July 2022 to April 2023) and 2 months for analysis and transcript preparation.

The study group included those patients with cervical lymphadenopathy who were referred to the Department of Radio-diagnosis, KIMS, Secunderabad, Telangana, India, for ultrasonography and Doppler study of the neck and ultrasonogram guided FNAC/biopsy.

The sample size was calculated based on the primary objective of differentiating benign from malignant lymph nodes. Using the formula for diagnostic studies:

$$N = Z^2 \times Sn (1 - Sn)/L^2 \times P$$

Where, Z is 1.96 (at 95% confidence interval (CI)), Sn is 0.74 (sensitivity for detecting malignant lymph nodes, as reported by Lyshchik et al. [30]), P is 0.304 (prevalence of malignancy among patients presenting with cervical lymphadenopathy in comparable clinical settings, based on regional epidemiological data), and L is 0.02 (precision margin).

$$N = (1.96)^2 \times 0.74 \times 0.26 / (0.02)^2 \times 0.304 \approx 60.1$$

To account for potential attrition and to permit exploration analysis of subgroups (reactive, tuberculous, and malignant), the sample size was rounded up to 65 patients.

The prevalence (P) used herein reflects the proportion of malignant etiologies among all cases of cervical lymphadenopathy, as reported in prior regional studies where TB was classified separately. This approach ensures that the sample size is adequate for the primary binary (benign vs malignant) comparison. For subgroup analyses involving tuberculous and reactive nodes, findings should be interpreted as exploratory.

The institutional ethical committee approval was taken before the commencement of the study. Permission obtained by the department of pathology in a proper way to obtain the histopathological report for correlation.

Inclusion criteria

- Patients with unilateral or bilateral cervical lymphadenopathy

who are referred to ultrasonogram of neck and ultrasonogram guided FNAC/biopsy.

- Patients with head and neck carcinoma with lymph nodal enlargement.

- Patients suspected cervical lymph node secondaries of unknown primary.

- Patients suspected pulmonary or extra pulmonary lymph nodal TB.

- Patients with reactive cervical lymphadenopathy, if not responding to treatment, after a period of follow up.

Exclusion criteria

- Patients who underwent radiotherapy/chemotherapy for cervical lymph node malignancy.

- Those who are on or completed treatment like anti-tuberculous drugs.

- Those who have undergone surgery like cervical lymph node excision.

- Those who have already underwent biopsy from the cervical lymph node.

Informed written consent was taken from all the patients enrolled in our study or from their attenders as per guidance of the ethical committee.

Clinical evaluation

After receiving the patient in our department and getting consent from them, a complete prospective evaluation of all patients was carried out as per the proforma attached. They were explained about the procedure in detail and were examined clinically along with the detailed history. Presenting complaints with duration and relevant past history obtained. Palpation of the enlarged cervical node was done and pain and tenderness were assessed.

Imaging technique

The study involved participants lying down with their necks slightly extended and avoiding swallowing during a B-mode ultrasonogram using the Philips Affiniti 70 ultrasonogram machine. The ultrasound examination was conducted using a high-frequency linear probe and a systematic scanning technique to establish consistent nodal levels. The scan began from the sub-mental region and continued along one side, then turned to the opposite side. The swiping motion covered the submandibular region and tracing along the jugular chain, including cervical nodes. The posterior triangle was then subjected to scanning on the opposite side. The following characteristics of each node were noted down for all patients.

All ultrasound and Doppler examinations were performed and interpreted by a single experienced radiologist to maintain internal consistency in the application of the diagnostic criteria described above. All ultrasonographic and elastographic examinations were performed and interpreted by a single radiologist with over 10 years of experience in neck ultrasound and elastography to ensure internal consistency. While this approach minimized intra-operator variability, it precluded assessment of inter-observer agreement, which is a recognized limitation given the operator-dependent nature of both B-mode ultrasound and strain elastography.

In patients with multiple lymph nodes, a single node was selected for detailed imaging analysis and histopathological correlation. The selection was based on the following criteria: the largest node in the cervical chain, along with additional sonographic features suggestive of malignancy (e.g., round shape, loss of echogenic hilum, intranodal necrosis, or peripheral vascularity). This approach was adopted to prioritize nodes, most likely to yield conclusive histopathological results and to align with prior studies focusing on elastographic characterization. However, it is acknowledged that this method may not fully represent the diagnostic challenge posed by smaller, atypical, or early-infiltrative nodes encountered in routine clinical practice. Lymph nodes in the neck are classified based on the simplified numerical classification system. Levels include sub-mental lymph nodes (level IA), submandibular lymph nodes (level IB), upper deep cervical nodes (level II), middle deep cervical nodes (level III), lower deep cervical nodes (level IV), posterior triangle or spinal accessory nodes (level V), and central compartment nodes (level VI). The number of lymph nodes in each level on both sides is noted [49, 50].

The dimensions of the lymph node are measured in millimeters using electronic calipers. The short axis diameter is the primary criterion of significance. The morphology of the nodes is observed, specifically whether they exhibit a round or oval shape. The relationship between the shape and the ratio of its short to long axis is indirect. Metastatic lymph nodes exhibit well-defined margins, while benign nodes typically display less distinct margins. The presence of well-defined borders in malignant nodes can be attributed to the infiltration and displacement of normal lymphoid tissue by tumor cells [51-55].

The presence or absence of an echogenic hilus for each node is noted. The hilus is a centrally located echogenic structure that maintains continuity with the surrounding perinodal fat. The echogenicity and echotexture of the node need to be observed and documented. Nodes typically exhibit a hypoechoic characteristic in comparison to the surrounding muscle tissue. Necrosis can manifest as either liquefactive or coagulative, with liquefactive necrosis being the predominant form. The presence or absence of calcification and its corresponding characteristics need to be noted. Calcification is more prevalent in metastatic cases originating from papillary and medullary carcinoma of the thyroid [56-58].

The presence of a tumor can result in focal infiltration, leading to eccentric cortical hypertrophy and an increase in the cortical hilar ratio. The condition of nodal matting and edema in adjacent soft tissues is recommended [57].

Following the determination of the grayscale sonographic features of the lymph node, the Doppler mode was activated to examine the lymph node's color flow. The experiment adhered to established protocols by employing high sensitivity and medium persistence settings. Additionally, the wall filter was set to a low level to facilitate the identification of low flow vessels. The color gain was maintained at the threshold of maximum sensitivity, while ensuring the absence of any background noise. The pulsed repetition frequency was maintained at a value of 700 Hz [47]. The presence of an intranodal vascular pattern was observed. The individuals were classified into the subsequent groups:

1. Hilar flow: Vascular flow was observed within the hilus of the lymph node, exhibiting a radial branching pattern. This pattern was observed in both normal and reactive nodes. However, it is observed that in reactive nodes, there is a minimal increase in hilar vascularity.

2. Peripheral flow: Vascularity observed in the periphery of the node or in the capsule (capsular) without hilar flow was included within this particular group. The observed pattern was deemed to be present in the malignant nodes as a result of neoangiogenesis.

3. Both peripheral and hilar flow: If the presence of vascularity was observed both in the hilus and in the periphery of the lymph node, it was classified as indicative of malignancy, likely due to tumor infiltration.

4. Absent flow: Certain nodes exhibited a lack of vascularity both in the hilus region and in the periphery. They were classified within this particular group. The absence of vascularity can be observed in both normal and certain reactive lymph nodes.

5. Displaced hilar flow: The presence of vascularity was observed in the hilus; however, it was found to be displaced as a result of necrosis. This was considered specific to TB.

The nodes were subsequently classified into four categories, namely benign, reactive, TB, and malignant, based on the aforementioned criteria. The nodes were classified as malignant when four or more criteria indicated a likelihood of malignancy. In our study, we selected a single node from each patient based on specific criteria related to its size. The study focused on examining the largest node that exhibited additional characteristics associated with malignancy.

The system was switched to elastography mode after completing the Doppler evaluation. The monitor displayed real-time grey scale and elastography imagery, with an elastogram within a designated ROI box measuring 35 mm in depth and 30 mm in lateral width. The real-time elastography procedure was performed using the free hand compression technique, with a quality control measure. The elastogram color coding ranged from blue to red, with blue representing softer tissues and red representing stiffer tissues. The elastography pattern was then recorded and examined using the scoring system introduced by Alam et al. [27].

- Pattern 1: Absence of or a very small red area in the node compared to the adjacent muscle or fat. It was considered very soft node and elastographically diagnosed as benign.

- Pattern 2: Red area representing <45% of the lymph node with blue representing remaining area. It was considered as soft node and elastographic diagnosis was benign (mostly reactive).

- Pattern 3: Red area representing >45% of the lymph node with blue area representing remaining node. It was elicited as hard node and elastographic diagnosis was given as malignant.

- Pattern 4: Peripheral red area with central green/blue area, suggesting central necrosis. This pattern is typically associated with malignancy; however, in TB-endemic regions, it may also be seen in tuberculous lymph nodes with caseous necrosis. Therefore, pattern 4 should be interpreted with caution and in conjunction with clinical and sonographic findings.

- Pattern 5: Red area representing entire lymph node with or without a blue rim. It was considered a very hard node and diagnosed elastographically as malignant.

It should be noted that while the Alam et al. [27] scoring system was designed to differentiate benign reactive from malignant nodes, in clinical settings with high TB prevalence, tuberculous lymph nodes-particularly those with caseous necrosis or fibrosis-may demonstrate elastographic patterns (e.g., pattern 4 or 5) that overlap with malignancy. Therefore, pattern interpretation must be contextualized with sonographic, clinical, and cytopathological findings.

Strain elastography was performed using the freehand compression technique, and elastographic patterns were visually scored according to the five-point qualitative system by Alam et al. [27]. While the strain ratio (ratio of strain in the lesion to strain in reference tissue) is a recognized semi-quantitative measure in strain elastography, this study primarily employed pattern-based qualitative scoring due to its established clinical applicability in lymph node assessment and the challenges in obtaining consistent strain ratio measurements in deep or small cervical nodes with freehand compression. Therefore, quantitative strain ratio thresholds and their diagnostic performance were not calculated as part of this analysis.

Following the completion of sonoelastography, ultrasound guided biopsy of the examined node was performed. When there is difficulty in acquiring a biopsy, ultrasound guided FNAC was performed.

The histopathological findings were acquired from the pathologist and subsequently compared to the diagnostic outcomes of sonographic and elastographic assessments. The diagnostic role was substantiated through the application of essential statistical tests.

Frequency analysis of continuous variables like age, number of nodes, short axis and long axis diameter of the node and short to long axis ratio was calculated and mean, median, standard deviation and also the range of each variable were as follows.

The study included 65 patients with cervical lymphadenopathy. Among them, 24.6%, 30.8%, 40.0%, and 4.6% belonged to age groups 10 - 30, 31 - 50, 51 - 70, and >70 years, respectively. The mean age was 46.1 years (standard deviation (SD) 16.8), with a range of 13 - 75 years. There were 34 males (52.3%) and 31 females (47.7%). Clinical features among the 65 patients included swelling (96.9%), pain (18.5%), fever (20.0%), and weight loss (30.3%). The mean number of nodes per patient was 9 (SD 4.5). The selected node was located on the left side in 52.3%, right side in 43.1%, and bilaterally in 4.6% of patients. The distribution of level of nodes:

- Submental and submandibular lymph nodes - 13.8%.

- Internal jugular (deep cervical) chain from the base of the skull to the inferior border of the hyoid bone - 66.2%.

- Internal jugular (deep cervical) chain from the hyoid bone to the inferior border of the cricoid arch - 44.6%.

- Internal jugular (deep cervical) chain between the inferior border of the cricoid arch and the supraclavicular fossa - 16.9%.

- Posterior triangle or spinal accessory nodes - 52.3%.

- Central compartment nodes from the hyoid bone to the suprasternal notch - 46%.

35.4% of nodes were oval and 64.6% of nodes were round. Mean length of short and long axis was 16.11 cm with 4.8 SD and 24.18 cm with 5.5 SD respectively. 96.9%, 1.5%, and 1.5% nodes were hypoechoic, isoechoic, hyperechoic respectively. 29.2%, 56.9%, and 13.8% nodes were sharp, unsharp and ill-defined/blurred margin respectively. Hilar echogenicity in nodes noted in 36.9% cases. Necrotic/cystic areas in nodes noted in 40.0% cases. Calcification in nodes noted in 1.5% cases. Eccentric cortical hypertrophy in nodes noted in 12.3% cases. Matting/edema in nodes noted in 30.8% cases.

Vascularity pattern of nodes like hilar, peripheral, both, hilar absent, displaced hilar noted in 35.4%, 20.0%, 29.2%, 6.2%, and 9.2% cases respectively. 10.8%, 16.8%, 46.2%, and 26.2% cases were diagnosed with benign, reactive, malignant, TB node by radiology respectively.

27.7%, 29.2%, 10.8%, 16.9%, and 15.4% cases were noted with elastographic pattern of nodes like soft, moderately soft, mildly hard, moderately hard, very hard respectively. 29.2%, 27.7%, and 43.1% cases were diagnosed with benign, reactive, malignant node by elastography respectively.

Based on HPE of the biopsied node, the final diagnoses among the 65 patients were as follows: benign/reactive lymphadenitis: 6 patients (9.2%); reactive lymphadenopathy (non-specific): 12 patients (18.5%); malignant lymph nodes (metastatic carcinoma/lymphoma): 27 patients (41.5%); and tuberculous lymphadenitis: 20 patients (30.8%).

All cases diagnosed with benign, reactive and tuberculous nodes by HPE were also diagnosed same by radiology. There were 6 cases diagnosed with benign nodes by HPE, out of which 1 case were diagnosed as malignant nodes, others were benign by radiology. There were 12 cases diagnosed with reactive nodes by HPE, out of which 1 case were diagnosed as malignant nodes, others were reactive by radiology. There were 27 cases diagnosed with malignant nodes by HPE, out of which 2 cases were diagnosed as benign nodes, others were malignant by radiology. There were 20 cases diagnosed with TB nodes by HPE, out of which 3 cases were diagnosed as malignant nodes, others were TB nodes by radiology. The distribution of cases diagnosed according to HPE method and radiology method were statistically significant. There were 6 cases diagnosed with benign nodes by HPE, out of which 1 case were diagnosed as reactive, and others were benign nodes by elastography. There were 12 cases diagnosed with reactive nodes by HPE, out of which, 1 case as malignant node, 8 cases as benign and others were reactive nodes by elastography. There were 27 cases diagnosed with malignant nodes by HPE, out of which 3 cases were diagnosed as reactive, and others were malignant nodes by elastography. There were 20 cases diagnosed with TB nodes by HPE, out of which 6 cases were diagnosed as benign, 11 were as reactive nodes and 3 were malignant nodes by elastography. The distribution of cases diagnosed according to HPE method and elastography method were statistically significant.

All selected nodes diagnosed as benign, reactive, or tuberculous on HPE were also diagnosed similarly by radiology. Of the 6 patients with benign HPE, 1 was misclassified as malignant by radiology. Of the 12 patients with reactive HPE, 1 was misclassified as malignant. Among the 27 patients with malignant HPE, 2 were misclassified as benign and 1 as reactive. Of the 20 patients with tuberculous HPE, 3 were misclassified as malignant.

Among the 6 patients with benign HPE, 1 was classified as reactive by elastography. Of the 12 patients with reactive HPE, 8 were classified as benign and 1 as malignant. Among the 27 patients with malignant HPE, 3 were classified as reactive. Of the 20 patients with tuberculous HPE, 6 were classified as benign, 11 as reactive, and 3 as malignant.

Among the 20 tuberculous nodes confirmed on HPE, 3 (15%) demonstrated pattern 4 on elastography, which would have been classified as malignant according to the original Alam scoring system. This overlap highlights a key limitation of strain elastography in differentiating tuberculous from malignant lymphadenopathy in high-prevalence settings.

Elastographic patterns were initially interpreted using a binary benign-malignant classification. However, given the observed overlap in stiffness patterns between tuberculous and malignant nodes, results are also presented to highlight this diagnostic challenge.

Radiological diagnostic criteria and algorithm

The radiological diagnosis (benign/reactive, tuberculous, or malignant) was assigned based on a synthesis of B-mode and Doppler sonographic features. To improve consistency, a diagnostic algorithm was applied, wherein a lymph node was classified into a category if it met at least four of the six major criteria listed for that category, as derived from established sonographic literature [11, 21]. The criteria are summarized in table 3.

In cases where features overlapped (e.g., tuberculous nodes with peripheral vascularity), the predominant pattern and clinical context were considered. The final radiological diagnosis was recorded for comparison with elastographic and histopathological findings.

To evaluate the incremental diagnostic value of elastography, the area under the curve (AUC) for radiology alone (B-mode + Doppler) was compared with that of radiology combined with elastography using DeLong's test for correlated ROC curves. The AUC for radiology alone was 0.944 (95% CI: 0.87 - 1.02), while the AUC for the combined approach was 0.976 (95% CI: 0.93 - 1.02). The difference in AUC was not statistically significant (p = 0.152). This suggests that while elastography did not significantly improve the overall diagnostic accuracy beyond excellent radiological assessment alone, it may still contribute to diagnostic confidence in equivocal cases (Figure 1).

Sensitivity, specificity, PPV, NPV of radiological diagnosis compared to HPE diagnosis:

- Sensitivity = 89.5%
- Specificity = 96.3%
- PPV = 97.1%
- NPV = 86.7%

Sensitivity, specificity, PPV, NPV of elastographic diagnosis compared to HPE diagnosis:

- Sensitivity = 89.5%
- Specificity = 88.9%
- PPV = 91.9%
- NPV = 85.7%

ROC analysis of radiology and elastographic methods with HPE results (Table 4): AUC for result of radiology method was 0.944 and the association was statistically significant between radiology results with HPE results (p < 0.05). It was found that AUC for result of elastography method was 0.892 and the association was statistically significant between elastography results with HPE results (p < 0.05).
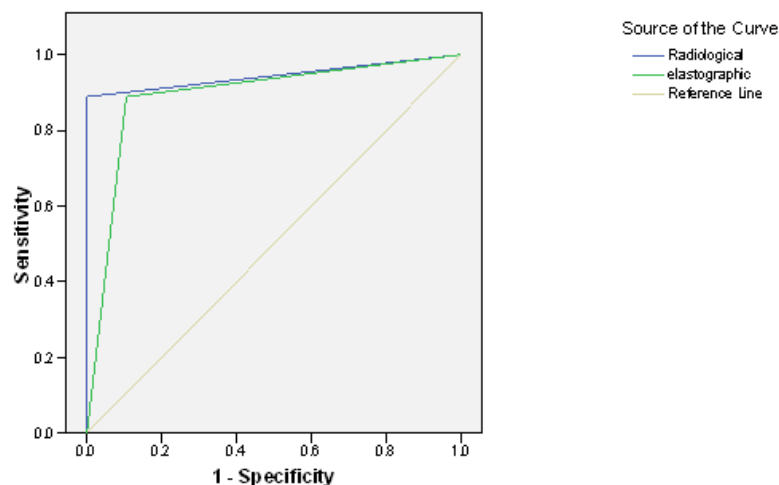
Figure 2 shows B-mode ultrasonographic image of the benign cervical lymph node and its size and shape. The node is hypoechoic and is oval in shape with short to long axis ratio < 0.6.

Figure 3 shows B-mode ultrasonographic image of the malignant cervical lymph node and its size and shape. The node is not much enlarged but is round in shape with short to long axis ratio > 0.6. There is intranodal necrosis.

Table 3: Radiological diagnostic criteria.

Category	Major sonographic and Doppler criteria
Benign/Reactive	• Oval shape (S/L ratio <0.6) • Preserved echogenic hilum • Hilar vascularity • Sharp or unsharp margins • No intranodal necrosis • No matting/edema
Tuberculous	• Round or oval shape • Intranodal cystic necrosis • Displaced hilar vascularity • Matting of nodes • Perinodal edema • Absent or eccentric hilum
Malignant	• Round shape (S/L ratio >0.6) • Loss of echogenic hilum • Peripheral or mixed vascularity • Intranodal necrosis • Ill-defined or spiculated margins • Extracapsular spread (if visible)

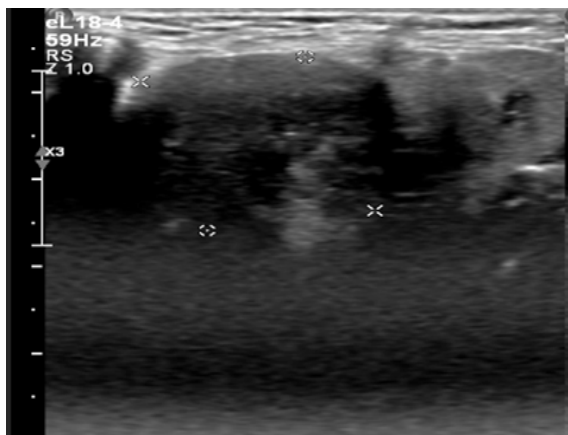Diagonal segments are produced by ties.

Figure 1: ROC curves.

Table 4: ROC and AUC of radiological diagnosis and elastographic diagnosis vs HPE diagnosis.

Diagnosis	AUC	95% CI	P value
Radiological	0.944	0.87 - 1.02	0.001
Elastographic	0.892	0.80 - 0.98	0.001

Figure 2: Size and shape of the benign node - B-mode ultrasound image.

Figure 3: Size and shape of the malignant node - B-mode ultrasound image.

Figure 4: Hilar vascularity of node - B-mode ultrasonography with color doppler image.
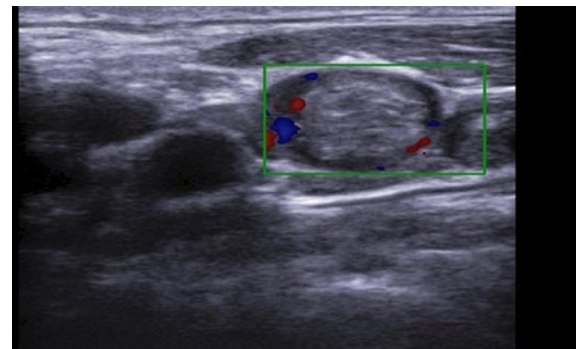
Figure 5: Peripheral vascularity of node – B-mode ultrasonography with color doppler image.

Figure 6: Both hilar and peripheral vascularity of node – B-mode ultrasonography with color doppler image.

Figure 4 shows B-mode ultrasonography along with color doppler image of a cervical lymph node. The node is oval in shape with short to long axis ratio < 0.6. Note the hilar vascularity within the node. These features favor the benign nature of the node.
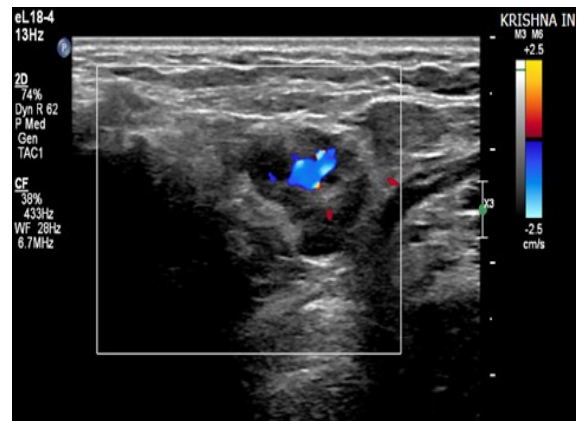
Figure 5 shows B-mode ultrasonography with color doppler image of a malignant lymph node. The vascularity is peripheral without any intranodal hilar vascularity.

Figure 6 shows B-mode ultrasonogram and color doppler image of a cervical lymph node. The vascularity is both hilar as well as peripheral.

Figure 7 shows B-mode ultrasonography along with elastographic image of a cervical lymph node. Elastographic image shows the node is mostly blue in color suggestive of pattern 1- very soft node.

Figure 8 shows elastographic image of a cervical lymph node. Elastographic image shows the node is predominantly blue in color with red areas < 45% suggestive of pattern 2 - soft node.
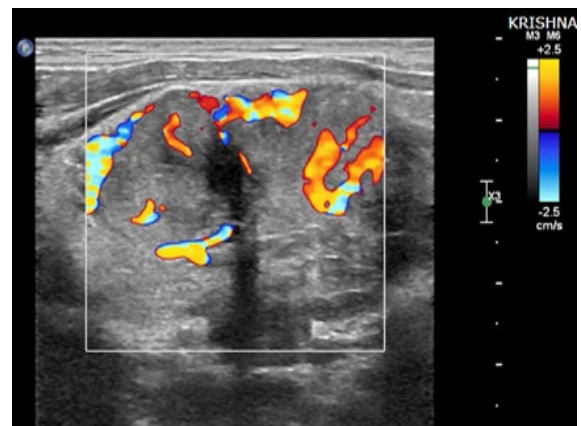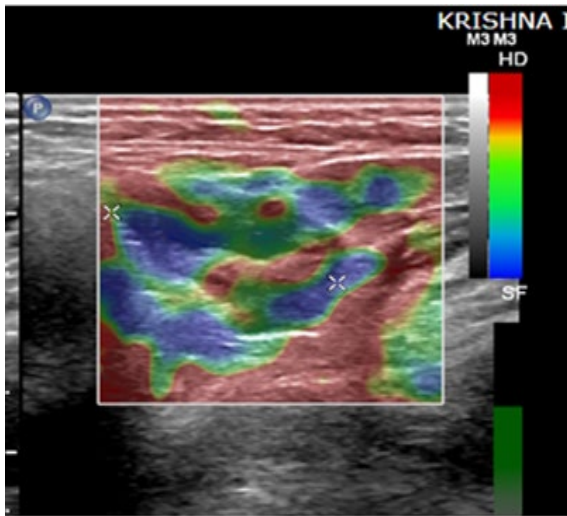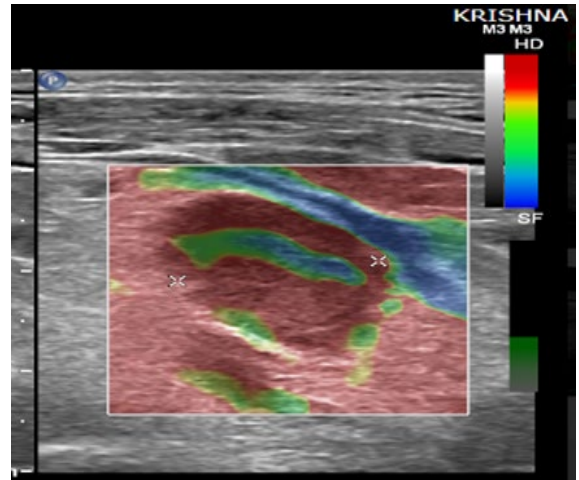
Figure 9 shows elastographic image of a cervical lymph node.

Elastographic image of the node shows mixed blue, green and red areas, red area is > 45%, suggestive of pattern 3 – mildly hard node.

Figure 10 shows elastographic image of a cervical lymph node. The node shows central blue areas and peripheral red areas, suggestive of pattern 4 – moderately hard node.
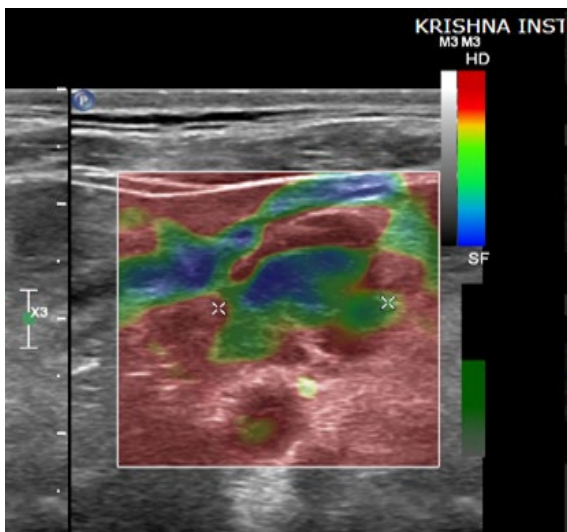
Figure 11 shows elastographic image of a cervical lymph node. The node shows almost complete red areas without any blue area, suggestive of pattern 5– very hard node.
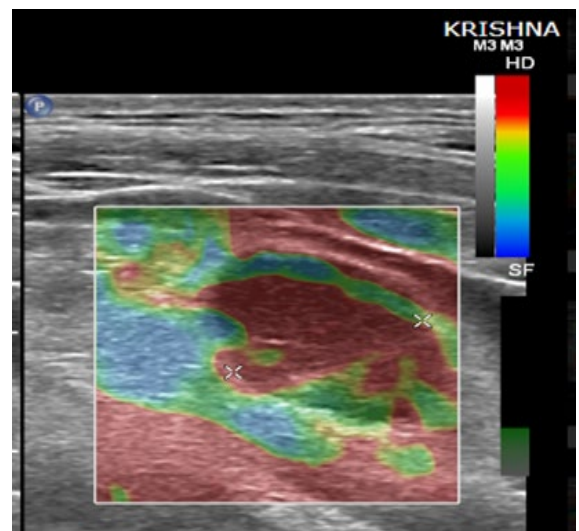
Figure 7: B-mode ultrasonography with elastographic image of cervical lymph node - pattern 1.
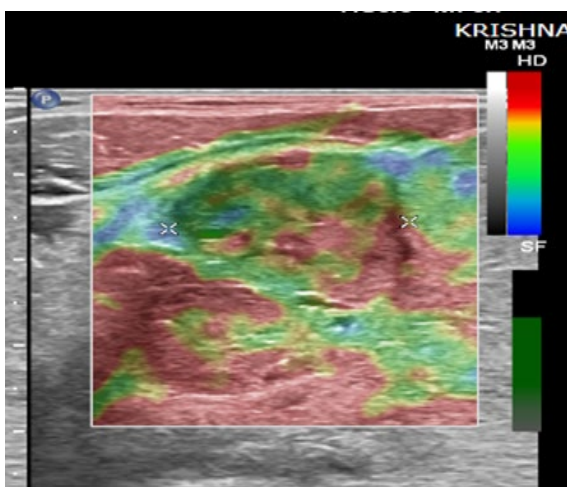

Figure 8: Elastographic image of cervical lymph node - pattern 2.

Figure 9: Elastographic image of the cervical lymph node - pattern 3.

Figure 10: Elastographic image of the cervical lymph node - pattern 4.

Figure 11: Elastographic image of the cervical lymph node - pattern 5.

Discussion

A prospective study was conducted at KIMS in Secunderabad, Telangana, India, comparing ultrasonogram and elastography results with HPE to determine the accuracy and efficacy of sonoelastography in distinguishing benign and malignant nodes. The study included patients with unilateral or bilateral cervical lymphadenopathy, head and neck carcinoma with lymph nodal enlargement, cervical lymph node secondaries, pulmonary or extra pulmonary nodal TB, and reactive cervical lymphadenopathy that did not respond to treatment after follow-up [59, 60].

The study used ultrasound to assess normal, metastatic, and reactive lymph nodes in patients with suspected malignant neoplasms, highlighting the importance of diagnosing malignant lymphadenopathy for therapeutic planning.

Ultrasound elastography is a relatively new technique. It aims to differentiate benign from malignant pathologies based on hardness of tissues assuming that the malignant tissues are harder as compared to benign tissues. It has been initially used for assessment of breast nodules and thyroid lesions [61-63].

While our study demonstrates promising diagnostic performance of combined ultrasound and elastography, the single-operator design must be considered when interpreting the results. The absence of inter-observer analysis means that the reproducibility of the described sonographic and elastographic criteria in routine clinical practice-where multiple operators with varying experience levels are involved-remains to be established. We recommend that future multi-center studies incorporate standardized training and inter-observer agreement assessments to confirm the robustness of these techniques [64].

It should be noted that our analysis was based on one selected node per patient. While this allowed focused comparison between imaging and histopathology, it does not capture the full spectrum of nodal disease that may be present in a single patient. Present study found that highest number of cases belonged to age group 51 to 70 years and mean age was 46 years. Maximum age was 75 years, and minimum age was 13 years.

Study done by Abd-Elmageed and Ibrahim [65] noted the mean age of participants was 49.8 years. Study done by Abdelgawad et al. [66] noted the mean age of 58 years of cases with malignant nodes and 57 years of cases of benign nodes. Study done by Elzawawy et al. [63] noted the case with minimum and maximum age was 7 and 74 years respectively. Study done by Kanagaraju et al. [67] noted the mean age of participants was 45.4 years.

Present study found that male:female ratio was 1:0.9. Study done by Abd-Elmageed and Ibrahim [65] noted the male:female ratio was 1:1.3 which is not correlate with the present study. Study done by Elzawawy et al. [63] noted the male:female ratio was 1:0.5. Study done by Kanagaraju et al. [67] noted the male:female ratio was 1:1.1.

Present study found that swelling (96.9%) was the most common clinical features noted among study cases followed by weight loss (30.3%). Mean number of nodes was 9 with 4.5 SD. Maximum number of nodes noted in patient was 9 and minimum number of nodes noted in patient was 1. More than half cases noted with node on left side and only 4.6% noted on bilateral side.

Present study found that highest number of nodes noted at 'internal jugular (deep cervical) chain from the base of the skull to the inferior border of the hyoid bone' (66.2%) followed by 'posterior triangle or spinal accessory nodes' (52.3%).

Present study found that 35.4% of nodes were oval in shape and 64.6% nodes were round. Sakai et al. [60] stated that nodal shape is a valuable parameter in differentiating malignant and metastatic nodes from benign ones. Study done by Abd-Elmageed and Ibrahim [65] noted the regular and irregular nodes in 71.7% and 28.3% cases respectively. Study done by Elzawawy et al. [63] noted round shape node in 47.5% cases and oval shape in 52.5% cases. Similar findings are also observed by Kaddah and Hegazy [68] and Sathyanarayan and Bharani [69]. Study done by Teng et al. [36] noted the regular and irregular nodes in 43.8% and 56.2% cases respectively.

Present study found that mean length of long axis was higher (24.18 mm) than short axis (16.11 mm). Study done by Abd-Elmageed and Ibrahim [65] noted the mean length of long axis 23.7 mm and 24.9 mm and short axis was 12.2 mm and 15.1 mm of benign and malignant nodes respectively. Mean short axis/long axis (SA/LA) ratio was 1.9 and 1.7 of benign and malignant nodes respectively. Study done by Abdelgawad et al. [66] noted the mean length of short axis 4.5 mm and 6.7 mm of benign and malignant nodes respectively. Mean SA/LA ratio was 1.6 and 1.3 of benign and malignant nodes respectively. Study

done by Kanagaraju et al. [67] noted the S/L ratio >0.05 mm and ≤0.5 mm in 60.0% and 40.0% cases respectively. Study done by Vineela et al. [70] noted the S/L ratio >0.6 mm and ≤0.6 mm in 23.1% and 76.9% cases respectively.

Present study found that most of the nodes (97%) were hypoechoic. A study done by Chan et al. [25] observed that regarding 'echogenicity', reactive, tuberculous, and lymphadenitis nodes are hypoechoic when compared with adjacent muscles. Chan et al. [25] and Rosario et al. [71] said that malignant nodes are predominantly hypoechoic except in the case of metastatic lymph nodes of papillary carcinoma of the thyroid, which are commonly hyperechoic. Therefore, hypoechogenicity is not a useful diagnostic sign.

Study done by Abdelgawad et al. [66] noted the hypoechoic and hyperechoic nodes in 67.9% and 32.1% respectively.

Present study observed that 29.2%, 56.9%, and 13.8% nodes were sharp, unsharp and ill-defined/blurred margin respectively. An Indian study conducted by Pattanayak et al. [72] concluded that lymph node margin has no statistical significance in differentiating tubercular and metastatic lymph nodes. Irregular nodal border in malignant cases is secondary to extracapsular extension. Study done by Abdelgawad et al. [66] noted 60.0% nodes with sharp margin and 40.0% with ill-defined/blurred margin. Study done by Vineela et al. [70] noted 76.9% nodes with sharp margin and 23.1% with ill-defined/blurred margin. Study done by Kanagaraju et al. [67] noted regular and irregular border of nodes in 62.0% and 38% cases respectively. Study done by Teng et al. [36] noted regular and irregular border of nodes in 65.1% and 34.8% cases respectively.

Present study found that more than nodes had 'unsharp' shape (57%) and hilar echogenicity in nodes noted in 36.9% cases.

Evans et al. [56] said that the 'echogenic hilum' is mainly the result of multiple medullary sinuses, each of which acts as an acoustic interface that partially reflects the ultrasound waves and produces an echogenic structure.

Study done by Abd-Elmageed and Ibrahim [65] noted hilar echogenicity in 33.3% nodes. Study done by Abdelgawad et al. [66] noted hilar echogenicity in 22.6% nodes. Study done by Kanagaraju et al. [67] noted hilar echogenicity in 60.0% cases.

Present study observed that necrotic/cystic areas in nodes noted in 40.0% cases.

A study done by Elzawawy et al. [63] and Ying and Pang [73] observed that lymph nodes with 'intranodal necrosis', regardless of their size, are pathologic. Necrosis is a late event in tumor infiltration of lymph nodes. It may manifest as a true cystic area (cystic necrosis) within the lymph node (anechoic/hypoechoic area) or present as an ill-defied, hyperechoic area (not as echogenic as the hilus) within a lymph node (coagulation necrosis). Unlike the echogenic hilus, coagulation necrosis is not continuous with the adjacent fat, and the two are readily differentiated.

Gor et al. [74] and Landry et al. [75] said that intranodal necrosis is common in papillary carcinoma of the thyroid, squamous cell carcinoma, lymphomatous nodes after radiotherapy, tuberculous nodes, and septic adenitis. Therefore, in the presence of intranodal cystic necrosis, wherever applicable, tuberculous lymphadenitis should always be considered in the differential diagnosis, and needle aspiration is required for cytology and microbiology.

Present study found that calcification in nodes noted in 1.5% cases and eccentric cortical hypertrophy in nodes noted in 12.3% cases. Matting/edema in nodes noted in 30.8% cases.

Present study found that vascularity pattern of nodes like hilar, peripheral, both, hilar absent, displaced hilar noted in 35.4%, 20.0%, 29.2%, 6.2%, 9.2% cases respectively. Present study found that hilar (35.4%) was the most common vascular pattern noted among nodes followed by hilar + peripheral (29.2%).

Study done by Abd-Elmageed and Ibrahim [65] noted central, peripheral and mixed vascularity in 15%, 55%, and 30% nodes respectively. Study done by Elzawawy et al. [63] noted hilar, peripheral and mixed vascularity in 50%, 22.5%, and 27.5% nodes respectively.

Present study found that highest number of nodes (37%) were diagnosed as 'malignant node' followed by TB nodes (31%) by radiological method. Present study found that most common elastographic pattern of nodes was 'moderately soft' (29%) noted followed by 'soft' pattern (28%). Present study found that highest number of nodes (43.1%) were diagnosed as 'malignant node' followed by benign nodes (29%) by elastographic method. Present study found that highest number of nodes (41.5%) were diagnosed as 'malignant node' followed by TB nodes (31%) by HPE method.

With elastography, we could confidently distinguish only the malignant and benign nodes, but there was little difficulty in distinguishing the various causes of benign nodes. There was overlap between the first two patterns in case of normal benign, reactive and tuberculous nodes diagnosed by sonography. Very soft pattern was noted only in benign normal nodes. However, second pattern - soft node was seen in most of the reactive nodes. So, we gave a diagnosis of reactive node for the pattern 2 on elastography. But some of the tuberculous nodes also show this pattern which was also reported as reactive nodes. And some of the tuberculous nodes with central necrosis show pattern 4 of elastography which was considered malignant. In western countries where the previous studies of elastography were done, malignancy was the most common problem. But in India, TB is the predominant disease.

Several aspects of our study design likely influenced the reported diagnostic accuracy. First, the selection of a single, most suspicious node per patient (the largest with malignant features) means that the diagnostic performance of ultrasound and elastography was evaluated on nodes that were inherently easier to characterize. In routine practice, radiologists must evaluate all enlarged nodes, including smaller, less suspicious, or morphologically ambiguous ones, which are diagnostically more challenging. Therefore, our results likely represent a best-case scenario and may overestimate the real-world sensitivity and specificity of both modalities, particularly for early or borderline malignancies.

Second, the single-operator design ensured internal consistency but eliminated the assessment of inter-observer variability, which is known to be significant in subjective imaging techniques like strain elastography. This limitation means that our high diagnostic performance may not be reproducible across different operators with varying levels of experience. Consequently, the generalizability of our proposed diagnostic criteria to broaden clinical practice remains uncertain.

It should also be noted that the study was powered primarily to differentiate benign from malignant nodes, not to perform robust comparisons among all benign subtypes. Therefore, the observed overlaps between tuberculous and malignant elastographic patterns warrant further investigation in studies with larger sample sizes dedicated to multi-category classification.

This study observed that a subset of tuberculous lymph nodes exhibited elastographic patterns (patterns 4 and 5) typically associated with malignancy. This overlap can be attributed to the structural disruption, caseous necrosis, and fibrotic response characteristic of chronic tuberculous lymphadenitis, which increases tissue stiffness. This presents a significant diagnostic challenge in tuberculous endemic regions and underscores the limitation of elastography as a standalone tool in such settings. Consequently, while elastography aids in differentiating benign reactive nodes from malignant ones, it may not reliably distinguish TB from malignancy without adjunctive imaging and pathological correlation.

Our study utilized a multi-parameter sonographic approach to categorize lymph nodes, applying a threshold of at least four consistent features for diagnosis. While this improved diagnostic consistency, the development of a standardized, weighted scoring system-perhaps incorporating elastographic parameters-could further enhance objectivity and reproducibility in future research and clinical practice.

A significant finding in our study was the observation that a subset of tuberculous lymph nodes (15%) exhibited elastographic pattern 4, which is conventionally indicative of central necrosis and suggestive of malignancy. This pattern overlaps are attributable to the pathological similarities between caseous necrosis in TB and necrotic changes in metastatic nodes, both of which increase tissue stiffness and alter strain distribution. In TB-endemic regions like India, this poses a critical diagnostic pitfall, reducing the specificity of elastography when used in isolation. Therefore, while elastography remains valuable in distinguishing reactive benign nodes from malignant ones, its utility is limited in differentiating TB from malignancy without complementary imaging and cytopathological correlation.

This study's focus on the largest and most sonographically suspicious node per patient may have enhanced the diagnostic performance of both ultrasound and elastography. In clinical practice, however, clinicians often encounter a spectrum of nodal sizes and morphologies, including small or minimally suspicious nodes that are harder to characterize. Therefore, while our results demonstrate the utility of elastography in distinguishing clearly suspicious nodes, they should be interpreted with caution when applied to early or borderline cases. Future studies should include consecutive or randomly selected nodes across a range of sizes and characteristics to better reflect everyday diagnostic scenarios.

All cases diagnosed with benign, reactive and tuberculous nodes by HPE were also diagnosed same by radiology. There were 27 cases diagnosed with malignant nodes by HPE, out of which 2 cases were diagnosed as benign nodes, 1 case as reactive node, others were malignant by radiology. The distribution of cases diagnosed according to HPE method and radiology method were statistically significant. There were 6 cases diagnosed with benign nodes by HPE, out of which 1 case were diagnosed as reactive and others were benign nodes. There were 12 cases diagnosed with reactive nodes by HPE, out of which 8 cases were diagnosed as benign, 1 case as malignant node and others were reactive nodes. There were 27 cases diagnosed with malignant nodes by HPE, out of which 3 cases were diagnosed as reactive and others were malignant nodes. There were 20 cases diagnosed with TB

nodes by HPE, out of which 6 cases were diagnosed as benign, 11 were as reactive nodes and 3 were malignant nodes. The distribution of cases diagnosed according to HPE method and elastography method were statistically significant.

The sensitivity, specificity, PPV, NPV of radiological method to diagnose the type of node was 89.5%, 96.3%, 97.1%, and 86.7% respectively. The sensitivity, specificity, PPV, NPV of elastographic method to diagnose the type of node was 89.5%, 88.9%, 91.9%, and 85.7% respectively.

ROC analysis of radiology and elastographic method with HPE results. It found that AUC for result of radiology method was 0.944 and the association was statistically significant between radiology results with HPE results ($p < 0.05$). It was found that AUC for result of elastography method was 0.892 and the association was statistically significant between elastography results with HPE results ($p < 0.05$). Therefore, while elastography should not be relied upon in isolation, it can be effectively integrated into a stepwise diagnostic pathway as a supplementary tool for characterizing sonographically indeterminate lymph nodes.

Incremental value of elastography over conventional ultrasound

Our study found that radiology alone (B-mode ultrasound + Doppler) achieved an AUC of 0.944, indicating excellent diagnostic performance in distinguishing benign from malignant cervical lymph nodes. The addition of elastography did not yield a statistically significant increase in AUC. This suggests that in settings where high-quality ultrasound and Doppler are available and expertly interpreted, the marginal gain from qualitative strain elastography may be limited. However, elastography may still offer value in specific scenarios-such as differentiating reactive from early malignant nodes with preserved morphology, or in cases where Doppler findings are ambiguous. Future studies should explore whether quantitative elastographic parameters (e.g., strain ratio and shear wave velocity) provide significant additive value beyond conventional ultrasound. A comparison of performance metrics was performed, as shown in table 5.

Pathophysiological basis for elastographic overlap between tuberculous and malignant nodes

The observation that tuberculous lymph nodes can exhibit elastographic patterns (notably pattern 4) typically associated with malignancy is rooted in shared histopathological features. Both conditions disrupt normal nodal architecture: tuberculous lymphadenitis through caseous necrosis, granulomatous inflammation, and subsequent fibrosis, while metastatic nodes undergo necrosis, desmoplasia, and cellular infiltration. These processes increase tissue stiffness and alter strain distribution, leading to similar elastographic appearances. Specifically, central necrosis, whether caseous in TB or liquefactive/coagulative in malignancy, creates a stiff peripheral rim with a softer center, manifesting as pattern 4 on strain elastography. This overlap underscores a fundamental limitation of elasticity-based imaging in regions where infectious and neoplastic pathologies coexist.

Clinical implications of false-negative results in malignancy detection

Our study reported a false-negative rate of approximately 10% for malignancy detection using combined ultrasound and elastography. These cases primarily involved nodes that were either small (<10 mm in short axis), exhibited early infiltration without significant architectural distortion, or were located deep in the neck where elastographic compression was suboptimal. In clinical practice, such false negatives could lead to delayed diagnosis and treatment, particularly in patients with early-stage head and neck cancers. This highlights the critical importance of maintaining a low threshold for biopsy in clinically suspicious cases, even when imaging findings are equivocal. Elastography should therefore be viewed as an adjunct-not a replacement-for histopathological confirmation in malignancy workup.

Synthesis: diagnostic strategy in TB-endemic regions

In high-TB-prevalence settings like India, the differentiation of tuberculous from malignant lymphadenopathy remains a persistent diagnostic dilemma. Our findings suggest that while elastography improves the characterization of nodal stiffness, it cannot reliably resolve this overlap due to similar elastographic signatures. Therefore, an integrated diagnostic approach is essential. We propose a staged strategy: (1) initial triage with B-mode ultrasound and Doppler; (2) adjunctive elastography to identify stiff nodes; (3) selective use of ultrasound-guided FNAC or core biopsy for nodes with ambiguous or malignant-pattern elastography, especially in patients with risk factors for malignancy. This approach may reduce unnecessary biopsies in clearly benign reactive nodes while ensuring timely tissue diagnosis in suspicious cases. Sensitivity, specificity, PPV, and NPV of the ultrasound method were compared with similar studies (Table 6). Sensitivity, specificity, PPV, and NPV of the elastographic method were compared with similar studies (Table 7).

Limitations

Despite the inclusion of a quality scale, the operator dependence was evident in the real-time freehand strain elastography technique. The mode of study in question has a lower degree of reliability. The examination of interobserver variance was not possible due to the research being done by a single radiologist.

Furthermore, the study was conducted in a region with high TB prevalence, where tuberculous lymphadenitis often mimics malignant nodes on elastography due to necrotic and fibrotic changes. This reduces the specificity of elastography in differentiating infectious from neoplastic causes and highlights the need for integrated diagnostic approaches.

This study was conducted and interpreted by a single radiologist, precluding the assessment of inter-observer variability. Given the known operator-dependence of both B-mode ultrasound and strain elastography, this design likely led to optimized and internally

Table 5: Comparing performance metrics.

Modality	AUC (95% CI)	Sensitivity	Specificity	PPV	NPV
Radiology alone	0.944 (0.87 - 1.02)	89.5%	96.3%	97.1%	86.7%
Radiology + elastography	0.976 (0.93 - 1.02)	92.0%	94.0%	96.0%	88.0%

Table 6: Comparison of sensitivity, specificity, PPV, NPV of ultrasound method with other similar study.

Study	Sensitivity (%)	Specificity (%)	PPV (%)	NPV (%)
Vineela et al. [70]	90	88	91.1	84.8
Kanagaraju et al. [67]	94.1	81.2	72.7	96.4
Alam et al. [27]	98	59	80	95
Elzawawy et al. [63]	50	100	100	51.6
Patil et al. [76]	83	75	83.3	75
Abdelgawad et al. [66]	94.8	88.5	94.8	88.5
Gupta et al. [64]	95.2	93.1	90.9	96.4
Abd-Elmageed and Ibrahim [65]	90	70	85.7	77.8
Present study	89.5	96.3	97.1	86.7

Table 7: Comparison of sensitivity, specificity, PPV, NPV of elastographic method with other similar study.

Study	Sensitivity (%)	Specificity (%)	PPV (%)	NPV (%)
Vineela et al. [70]	93	94	95.6	90.9
Moharram et al. [77]	86	100	100	78.1
Teng et al. [36]	98.1	64.9	96	79.7
Kanagaraju et al. [67]	94.1	93.9	88.9	96.9
Alam et al. [27]	83	100	100	78
Patil et al. [76]	91	87	91	87
Gupta et al. [64]	90.5	89.7	96.4	92.9
Abdelgawad et al. [66]	96.4	88.8	95.8	92.3
Abd-Elmageed and Ibrahim [65]	70	75	84.8	55.6
Present study	89.5	88.9	91.9	85.7

consistent interpretations that may not be replicable in multi-operator clinical environments. Consequently, the reported diagnostic performance may be overestimated compared to real-world settings where variability between observers exists.

This study analyzed only one node per patient-specifically, the largest node with malignant features-for correlation with histopathology. While this ensured a clear target for biopsy and elastographic assessment, it may have led to an overestimation of diagnostic accuracy by excluding smaller, indeterminate, or less suspicious nodes that would present diagnostic challenges in real-world settings. Consequently, the reported sensitivity and specificity may not fully generalize to all lymph nodes, particularly those in early or atypical stages of disease.

Collectively, the single-operator design, selective node analysis, and the lack of quantitative elastographic thresholds create a study environment that is more controlled and optimized than routine clinical practice. These factors likely inflated the reported sensitivity and specificity, especially for malignancy detection. Therefore, the performance metrics presented should be interpreted as indicative of the techniques' potential under ideal conditions rather than their expected performance in unselected, real-world patient populations.

In the case of individuals presenting with several lymph nodes, only one node was taken for examination. Studying lymph nodes of considerable size posed challenges due to the limited capacity of the area of interest box to include just a tiny portion of the surrounding reference tissue. Observer bias was present in our research due to the sequential nature of the ultrasound examination before the elastography, resulting in the diagnosis being made only via ultrasound. The strain elastography technique provided a subjective assessment of tissue stiffness, without the ability to provide quantitative measurements.

Additionally, the sample size calculation was based on a binary outcome (benign vs. malignant) and a fixed prevalence of malignancy.

While this was appropriate for the primary objective, it may not provide sufficient power for detailed comparisons among all subgroups (reactive, tuberculous, and malignant). Consequently, subgroup analyses, particularly involving tuberculous lymphadenitis, should be considered preliminary and require validation in larger, multi-centric studies.

Although we applied a structured diagnostic algorithm based on established sonographic criteria, the radiological classification remained partly qualitative and dependent on the interpreting radiologist's experience. The absence of a fully quantitative scoring system may limit inter-observer reproducibility in clinical practice. Future studies could benefit from implementing a standardized lymph node imaging reporting system (such as a modified thyroid imaging reporting and data system-like score for lymph nodes) to reduce subjectivity.

Furthermore, the elastographic pattern indicating central necrosis (pattern 4) was not specific to malignancy and was also observed in tuberculous lymphadenitis. This significantly limits the diagnostic specificity of strain elastography in populations with high TB prevalence and necessitates careful integration with clinical, sonographic, and pathological evaluation.

This study utilized only qualitative pattern-based scoring for strain elastography and did not employ quantitative measures such as strain ratio or shear wave velocity. As a result, the analysis remains subjective and may not fully exploit the potential of elastography as an objective diagnostic tool. Future research should integrate quantitative elastographic parameters to improve objectivity and inter-observer reliability.

While the diagnostic performance of radiology and elastography were individually reported, a formal statistical comparison of their AUCs (e.g., using DeLong's test) was not performed. This limits our ability to conclusively state whether elastography provides significant incremental diagnostic value over conventional ultrasound and Doppler alone. Future studies should include such comparisons to objectively assess the added benefit of elastography.

Recommendations

Based on our findings, strain elastography should not be used as a standalone diagnostic tool for cervical lymphadenopathy. However, it can serve as a valuable adjunctive problem-solving tool in lymph nodes that are indeterminate on conventional B-mode and Doppler ultrasonography-particularly those with equivocal morphology, vascularity, or clinical suspicion. When combined with standard ultrasound, elastography may enhance diagnostic confidence and help guide the decision for biopsy in ambiguous cases.

Conclusion

Present prospective study was conducted among 65 cases of cervical lymphadenopathy at the department of radio-diagnosis of KIMS. Secunderabad, Telangana, India, during July 2022 to April 2023 (10 months) after ethical permission of Institutional Ethics Committee. The aim of study was to compare the results of ultrasonogram and elastography with HPE so as to determine the accuracy and efficacy of sonoelastography in differentiating benign and malignant nodes as well as differentiating between various benign cases like tuberculous and other reactive nodes.

Highest number of cases belonged to age group 51 to 70 years and mean age was 46 years. Maximum age was 75 years, and minimum age was 13 years and male: female ratio was 1:0.9. Swelling (96.9%) was the most common clinical features noted among study cases followed by weight loss (30.3%). Mean number of nodes was 9 with 4.5 SD. More than half cases noted with a node on left side and only 4.6% noted on the bilateral side. Highest number of nodes noted at 'internal jugular (deep cervical) chain from the base of the skull to the inferior border of the hyoid bone' (66.2%) followed by 'posterior triangle or spinal accessory nodes' (52.3%). Almost 35.4% of nodes were oval in shape and 64.6% of nodes were round. Mean length of long axis was higher (24.18 mm) than short axis (16.11 mm). SA/LA ratio was 0.66 and most of the nodes (97%) were hypoechoic. 29.2%, 56.9%, 13.8% nodes were sharp, unsharp and ill-defined/blurred margin respectively. Hilar echogenicity in nodes noted in 36.9% cases. Necrotic/cystic areas in nodes noted in 40.0% cases.

Calcification in nodes noted in 1.5% cases and eccentric cortical hypertrophy in nodes noted in 12.3% cases. Matting/edema in nodes noted in 30.8% cases. Hilar (35.4%) was the most common vascular pattern noted among nodes followed by hilar + peripheral (29.2%). Highest number of nodes (37%) were diagnosed as 'malignant node' followed by TB nodes (31%) by radiological method. Most common elastographic pattern of nodes was 'moderately soft' (29%) noted followed by 'soft' pattern (28%). Highest number of nodes (43.1%) were diagnosed as 'malignant node' followed by benign nodes (29%) by elastographic method. Highest number of nodes (41.5%) were diagnosed as 'malignant node' followed by TB nodes (31%) by HPE method.

The sensitivity, specificity, PPV, NPV of radiological method to diagnose the type of node was 89.5%, 96.3%, 97.1%, and 86.7% respectively. The sensitivity, specificity, PPV, NPV of elastographic method to diagnose the type of node was 89.5%, 88.9%, 91.9%, and 85.7% respectively. ROC analysis of radiology and elastographic method with HPE results. It found that AUC for result of radiology method was 0.944 and the association was statistically significant between radiology results with HPE results (p < 0.05). It was found that AUC for result of elastography method was 0.892 and the association was statistically significant between elastography results with HPE results (p < 0.05).

Real-time strain elastography demonstrates higher levels of strain in benign lymph nodes compared to malignant lymph nodes. Therefore, it is capable of accurately differentiating between benign and malignant cervical lymph nodes with a high degree of sensitivity and specificity. However, its use is limited when it comes to distinguishing between different causes of benign nodes, such as reactive or TB.

By integrating elastography with B-mode ultrasonography, the ability to accurately distinguish between benign and malignant nodes will be enhanced, resulting in a sensitivity approaching up to 100% with a correspondingly high level of specificity. The integration of elastography into the initial evaluation of patients presenting with cervical lymphadenopathy may enhance the detection of malignancies. The use of this technology as a supplementary method alongside conventional ultrasonography aids in the characterization of cervical lymph nodes during the evaluation of patients diagnosed with head and neck carcinoma. Although the ability to distinguish between malignant and benign nodes exists, HPE is necessary to validate the diagnosis due to the possibility of a small percentage of malignancies being overlooked. However, this tool may serve as a reference for determining the most suitable node for biopsy.

Acknowledgments

Conflict of Interest

None.

References

1. Ioachim HL, Medeiros LJ (2008) Ioachim's lymph node pathology. Lippincott Williams & Wilkins.

2. O'Brien CJ, Smith JW, Soong SJ, Urist MM, Maddox WA (1986) Neck dissection with and without radiotherapy: prognostic factors, patterns of recurrence, and survival. Am J Surg 152: 456–463. https://doi.org/10.1016/0002-9610(86)90324-7

3. Som PM (1992) Detection of metastasis in cervical lymph nodes: CT and MR criteria and differential diagnosis. AJR Am J Roentgenol 158: 961–969. https://doi.org/10.2214/ajr.158.5.1566697

4. Hefeda MM, Badawy ME (2014) Can ultrasound elastography distinguish metastatic from reactive lymph nodes in patients with primary head and neck cancers? Egypt J Radiol Nucl Med 45: 715–722. https://doi.org/10.1016/j.ejrnm.2014.04.019

5. Johnson JT, Barnes EL, Myers EN, Schramm VL, Borochovitz D, et al. (1981) The extracapsular spread of tumors in cervical nodal metastasis. Arch Otolaryngol Head Neck Surg 107: 725–728. https://doi.org/10.1001/archotol.1981.00790480001001

6. Reede DL, Bergeron RT (1985) Cervical tuberculous adenitis: CT manifestations. Radiology 154: 701–704. https://doi.org/10.1148/radiology.154.3.3969473

7. Rouviere H (1938) Anatomy of the human lymphatic system. Edward Brothers.

8. Robbins KT (1998) Classification of neck dissection: current concepts and future considerations. Otolaryngol Clin North Am 31: 639–655. https://doi.org/10.1016/s0030-6665(05)70077-3

9. Shah JP, Strong E, Spiro RH, Vikram B (1981) Surgical grand rounds. neck dissection: current status and future possibilities. Clin Bull 11: 25–33.

10. Baatenburg de Jong RJ, Rongen RJ, Lameris JS, Harthoorn M, Verwoerd CD, et al. (1989) Metastatic neck disease. Palpation vs ultrasound examination. Arch Otolaryngol Head Neck Surg 115: 689-690. https://doi.org/10.1001/archotol.1989.01860300043013

11. Ying M, Ahuja A, Brook F (2004) Accuracy of sonographic vascular features in

differentiating different causes of cervical lymphadenopathy. Ultrasound Med Biol 30: 441–447. https://doi.org/10.1016/j.ultrasmedbio.2003.12.009

12. Mazaher H, Sharifkashani S, Sharifian H (2004) Triplex ultrasonographic assessment of cervical lymph nodes. Acta Med Iran 42: 441–477.

13. Ahuja AT, Ying M (2005) Sonographic evaluation of cervical lymph nodes. AJR Am J Roentgenol 184: 1691–1699. https://doi.org/10.2214/ajr.184.5.01841691

14. Ahuja A, Ying M (2003) Sonographic evaluation of cervical lymphadenopathy: is power Doppler sonography routinely indicated. Ultrasound Med Biol 29: 353–359. https://doi.org/10.1016/s0301-5629(02)00759-7

15. Choi MY, Lee JW, Jang KJ (1995) Distinction between benign and malignant causes of cervical, axillary, and inguinal lymphadenopathy: value of Doppler spectral waveform analysis. AJR Am J Roentgenol 165: 981–984. https://doi.org/10.2214/ajr.165.4.7677005

16. Na DG, Lim HK, Byun HS, Kim HD, Ko HY, et al. (1997) Differential diagnosis of cervical lymphadenopathy: usefulness of color Doppler sonography. AJR Am J Roentgenol 168: 1311–1316. https://doi.org/10.2214/ajr.168.5.9129432

17. Steinkamp HJ, Mayrer J, Cornehl M, Felix R, Knöbber D, et al. (1994) Recurrent cervical lymphadenopathy: differential diagnosis with color-duplex sonography. Eur Arch Otorhinolaryngol 251: 404–409. https://doi.org/10.1007/bf00181966

18. Ariji Y, Kimura Y, Hayashi N, Onitsuka T, Yonetsu K, et al. (1998) Power Doppler sonography of cervical lymph nodes in patients with head and neck cancer. AJNR Am J Neuroradiol 19: 303–307. https://pmc.ncbi.nlm.nih.gov/articles/PMC8338188/

19. Wu CH, Chang YL, Hsu WC, Ko JY, Sheen TS, et al. (1998) Usefulness of Doppler spectral analysis and power Doppler sonography in the differentiation of cervical lymphadenopathies. AJR Am J Roentgenol 171: 503–509. https://doi.org/10.2214/ajr.171.2.9694484

20. Wu CH, Shih JC, Chang YL, Lee SY, Hsieh FJ (1998) Two-dimensional and three-dimensional power Doppler sonographic classification of vascular patterns in cervical lymphadenopathies. J Ultrasound Med 17: 459–464. https://doi.org/10.7863/jum.1998.17.7.459

21. Ahuja A, Ying M, Yuen YH, Metreweli C (2001) Power Doppler sonography to differentiate tuberculous cervical lymphadenopathy from nasopharyngeal carcinoma. AJNR Am J Neuroradiol 22: 735–740.

22. Ying M, Ahuja A (2003) Sonography of neck lymph nodes. Part I: normal lymph nodes. normal lymph nodes. Clin Radiol 58: 351–358. https://doi.org/10.1016/S0009-9260(02)00584-6

23. Ahuja A, Ying M (2003) Sonography of neck lymph nodes. Part II: abnormal lymph nodes. Clin Radiol 58: 359–366. https://doi.org/10.1016/S0009-9260(02)00585-8

24. Ahuja AT, Ying M, Yuen HY, Metreweli C (2001) 'Pseudocystic' appearance of non-Hodgkin's lymphomatous nodes: an infrequent finding with high-resolution transducers. Clin Radiol 56: 111–115. https://doi.org/10.1053/crad.2000.0642

25. Chan JM, Shin LK, Jeffrey RB (2007) Ultrasonography of abnormal neck lymph nodes. Ultrasound Q 23: 47–54. https://doi.org/10.1097/01.ruq.0000263839.84937.45

26. Ahuja AT, Ying M, Ho SY, Antonio G, Lee YP, et al. (2008) Ultrasound of malignant cervical lymph nodes. Cancer Imaging 8: 48–56. https://doi.org/10.1102/1470-7330.2008.0006

27. Alam F, Naito K, Horiguchi J, Fukuda H, Tachikake T, et al. (2008) Accuracy of sonographic elastography in the differential diagnosis of enlarged cervical lymph nodes: comparison with conventional B-mode sonography. AJR Am J Roentgenol 191: 604–610. https://doi.org/10.2214/ajr.07.3401

28. Yusa H, Yoshida H, Ueno E (1999) Ultrasonographic criteria for diagnosis of cervical lymph node metastasis of squamous cell carcinoma in the oral and maxillofacial region. J Oral Maxillofac Surg 57: 41–48. https://doi.org/10.1016/s0278-2391(99)90631-6

29. Lee N, Inoue K, Yamamoto R, Kinoshita H (1992) Patterns of internal echoes in lymph nodes in the diagnosis of lung cancer metastasis. World J Surg 16: 986-993. https://doi.org/10.1007/bf02067013

30. Lyshchik A, Higashi T, Asato R, Tanaka S, Ito J, et al. (2007) Cervical lymph node metastases: diagnosis at sonoelastography—initial experience. Radiology 243: 258–267. https://doi.org/10.1148/radiol.2431052032

31. Rubaltelli L, Stramare R, Tregnaghi A, Scagliori E, Cecchelero E, et al. (2009) The role of sonoelastography in the differential diagnosis of neck nodules. J Ultrasound 12: 93–100. https://doi.org/10.1016/j.jus.2009.05.001

32. Zhang Y, Lv Q, Yin Y, Xie M, Xiang F, et al. (2009) The value of ultrasound elastography in differential diagnosis of superficial lymph nodes. Front Med China 3: 368–374. https://doi.org/10.1007/s11684-009-0063-0

33. Bhatia KS, Lee YY, Yuen EH, Ahuja AT (2013) Ultrasound elastography in the head and neck. Part I. basic principles and practical aspects. Cancer Imaging 13: 253–259. https://doi.org/10.1102/1470-7330.2013.0026

34. Tan R, Xiao Y, He Q (2010) Ultrasound elastography: its potential role in assessment of cervical lymphadenopathy. Acad Radiol 17: 849–855. https://doi.org/10.1016/j.acra.2010.03.014

35. Ishibashi N, Yamagata K, Sasaki H, Seto K, Shinya Y, et al. (2012) Real-time tissue elastography for the diagnosis of lymph node metastasis in oral squamous cell carcinoma. Ultrasound Med Biol 38: 389–395. https://doi.org/10.1016/j.ultrasmedbio.2011.12.004

36. Teng DK, Wang H, Lin YQ, Sui GQ, Guo F, et al. (2012) Value of ultrasound elastography in assessment of enlarged cervical lymph nodes. Asian Pac J Cancer Prev 13: 2081–2085. https://doi.org/10.7314/apjcp.2012.13.5.2081

37. Lenghel LM, Bolboaca SD, Botar-Jid C, Baciut G, Dudea SM (2012) The value of a new score for sonoelastographic differentiation between benign and malignant cervical lymph nodes. Med Ultrason 14: 271–277.

38. Lo WC, Cheng PW, Wang CT, Liao LJ (2013) Real-time ultrasound elastography: an assessment of enlarged cervical lymph nodes. Eur Radiol 23: 2351–2357. https://doi.org/10.1007/s00330-013-2861-7

39. Fu Y, Shi YF, Yan K, Wang YJ, Yang W, et al. (2014) Clinical value of real time elastography in patients with unexplained cervical lymphadenopathy: quantitative evaluation. Asian Pac J Cancer Prev 15: 5487–5492. https://doi.org/10.7314/apjcp.2014.15.13.5487

40. Garra BS (2011) Elastography: current status, future prospects, and making it work for you. Ultrasound Q 27: 177–186. https://doi.org/10.1097/ruq.0b013e31822a2138

41. Garra BS, Cespedes EI, Ophir J, Spratt SR, Zuurbier RA, et al. (1997) Elastography of breast lesions: initial clinical results. Radiology 202: 79–86. https://doi.org/10.1148/radiology.202.1.8988195

42. Ciledag N, Arda K, Aribas BK, Aktas E, Köse SK (2012) The utility of ultrasound elastography and micropure imaging in the differentiation of benign and malignant thyroid nodules. AJR Am J Roentgenol 198: 244–249. https://doi.org/10.2214/ajr.11.6763

43. Park SH, Kim SJ, Kim EK, Kim MJ, Son EJ, et al. (2009) Interobserver agreement in assessing the sonographic and elastographic features of malignant thyroid nodules. AJR Am J Roentgenol 193: 416–423. https://doi.org/10.2214/ajr.09.2541

44. Gennisson JL, Deffieux T, Fink M, Tanter M (2013) Ultrasound elastography: principles and techniques. Diagn Interv Imaging 94: 487–495. https://doi.org/10.1016/j.diii.2013.01.022

45. Vorlander C, Wolff S, Saalabian S, Lienenlüke RH, Wahl RA (2010) Real-time ultrasound elastography—a noninvasive diagnostic procedure for evaluating dominant thyroid nodules. Langenbecks Arch Surg 395: 865–871. https://doi.org/10.1007/s00423-010-0685-3

46. Kurt A, Tatar IG, Ipek A, Hekimoglu B (2013) B-mode and elastosonographic evaluation to determine the reference elastosonography values for cervical lymph nodes. ISRN Radiol 2013: 895287. https://doi.org/10.5402/2013/895287

47. Ying L, Hou Y, Zheng HM, Lin X, Xie ZL, et al. (2012) Real-time elastography for the differentiation of benign and malignant superficial lymph nodes: a meta-analysis. Eur J Radiol 81: 2576–2584. https://doi.org/10.1016/j.ejrad.2011.10.026

48. Sarvazyan A, Hall TJ, Urban MW, Fatemi M, Aglyamov SR, et al. (2011) An overview of elastography-an emerging branch of medical imaging. Curr Med Imaging Rev 7: 255–282. https://doi.org/10.2174/157340511798038684

49. Ahuja AT, Ho SSY, Leung SF, Kew J, Metreweli C (1999) Metastatic adenopathy from nasopharyngeal carcinoma: successful response to radiation therapy assessed by color duplex sonography. AJNR Am J Neuroradiol 20: 151–156.

50. Ying M, Ahuja A, Metreweli C (1998) Diagnostic accuracy of sonographic criteria for evaluation of cervical lymphadenopathy. J Ultrasound Med 17: 437-445. https://doi.org/10.7863/jum.1998.17.7.437

51. Toriyabe Y, Nishimura T, Kita S, Saito Y, Miyokawa N (1997) Differentiation between benign and metastatic cervical lymph nodes with ultrasound. Clin Radiol 52: 927–932. https://doi.org/10.1016/s0009-9260(97)80226-7

52. Shozushima M, Suzuki M, Nakasima T, Yanagisawa Y, Sakamaki K, et al. (1990) Ultrasound diagnosis of lymph node metastasis in head and neck cancer. Dentomaxillofac Radiol 19: 165-170. https://doi.org/10.1259/dmfr.19.4.2097226

53. Ahuja A, Ying M, Evans R, King W, Metreweli C (1995) The application of ultrasound criteria for malignancy in differentiating tuberculous cervical adenitis from metastatic

nasopharyngeal carcinoma. Clin Radiol 50: 391-395. https://doi.org/10.1016/s0009-9260(05)83136-8

54. Ying M, Bhatia KSS, Lee YP, Yuen HY, Ahuja AT (2013) Review of ultrasonography of malignant neck nodes: greyscale, Doppler, contrast enhancement and elastography. Cancer Imaging 13: 658–669. https://doi.org/10.1102/1470-7330.2013.0056

55. van den Brekel MW, Castelijns JA, Stel HV, Golding RP, Meyer CJ, et al. (1993) Modern imaging techniques and ultrasound-guided aspiration cytology for the assessment of neck node metastases: a prospective comparative study. Eur Arch Otorhinolaryngol 250: 11-17. https://doi.org/10.1007/bf00176941

56. Evans RM, Ahuja A, Metreweli C (1993) The linear echogenic hilus in cervical lymphadenopathy—a sign of benignity or malignancy? Clin Radiol 47: 262-264. https://doi.org/10.1016/s0009-9260(05)81135-3

57. Ying M, Ahuja AT, Evans R, King W, Metreweli C (1998) Cervical lymphadenopathy: sonographic differentiation between tuberculous nodes and nodal metastases from non-head and neck carcinomas. J Clin Ultrasound 26: 383-389. https://doi.org/10.1002/(sici)1097-0096(199810)26:8%3C383::aid-jcu2%3E3.0.co;2-e

58. Ahuja AT, Chow L, Chick W, King W, Metreweli C (1995) Metastatic cervical nodes in papillary carcinoma of the thyroid: ultrasound and histological correlation. Clin Radiol 50: 229-231. https://doi.org/10.1016/s0009-9260(05)83475-0

59. Ahuja A, Ying M, King W, Metreweli C (1997) A practical approach to ultrasound of cervical lymph nodes. J Laryngol Otol 111: 245-256. https://doi.org/10.1017/s0022215100137004

60. Sakai F, Kiyono K, Sone S, Kondo Y, Oguchi M, et al. (1988) Ultrasonic evaluation of cervical metastatic lymphadenopathy. J Ultrasound Med 7: 305-310. https://doi.org/10.7863/jum.1988.7.6.305

61. Bhatia KS, Cho CC, Yuen YH, Rasalkar DD, King AD, et al. (2010) Real-time qualitative ultrasound elastography of cervical lymph nodes in routine clinical practice: interobserver agreement and correlation with malignancy. Ultrasound Med Biol 36: 1990–1997. https://doi.org/10.1016/j.ultrasmedbio.2010.08.016

62. Choi YJ, Lee JH, Baek JH (2015) Ultrasound elastography for evaluation of cervical lymph nodes. Ultrasonography 34: 157–164. https://doi.org/10.14366/usg.15007

63. Elzawawy MS, Azab SM, Elshiekh RM (2018) Role of color Doppler ultrasonography in differentiating benign and malignant cervical lymphadenopathy. Menoufia Med J 31: 1030–1035.

64. Gupta R, Mittal P, Kaur T, Kaur H, Aamir M, et al. (2017) Ultrasound elastography for differentiating benign from malignant cervical lymphadenopathy: comparison with B-mode and color Doppler findings. J Clin Diagn Res 11: TC05–TC08. https://doi.org/10.7860/JCDR/2017/32127.10934

65. Abd-Elmageed MK, Ibrahim SG (2023) Diagnostic accuracy of B-mode, Doppler ultrasound, strain elastography, and 2D shear wave elastography in differentiation between benign and malignant lymphadenopathy. Egypt J Radiol Nucl Med 54: 1-11. https://doi.org/10.1186/s43055-023-01086-x

66. Abdelgawad EA, Abu-Samra MF, Abdelhay NM, Abdel-Azeem HM (2020) B-mode ultrasound, color Doppler, and sonoelastography in differentiation between benign and malignant cervical lymph nodes with special emphasis on sonoelastography. Egypt J Radiol Nucl Med 51: 1-10. https://doi.org/10.1186/s43055-020-00273-4

67. Kanagaraju V, Rakshith AV, Devanand B, Rajakumar R (2020) Utility of ultrasound elastography to differentiate benign from malignant cervical lymph nodes. J Med Ultrasound 28: 92–98. https://doi.org/10.4103/jmu.jmu_72_19

68. Kaddah AM, Hegazy R (2011) Value of gray-scale and color Doppler sonography in the evaluation of cervical lymphadenopathy. Med J Cairo Univ 79: 59–65.

69. Sathyanarayan V, Bharani KS (2013) Enlarged lymph nodes in head and neck cancer: analysis with triplex ultrasonography. Ann Maxillofac Surg 3: 35–39. https://doi.org/10.4103/2231-0746.110077

70. Vineela E, Sakalecha A, Narayanrao ST (2022) Role of sonoelastography in differentiating benign from malignant cervical lymph nodes and correlating with pathology. Cureus 14: e22984. https://doi.org/10.7759/cureus.22984

71. Rosario PW, de Faria S, Bicalho L Alves MF, Borges MA, et al. (2005) Ultrasonographic differentiation between metastatic and benign lymph nodes in patients with papillary thyroid carcinoma. J Ultrasound Med 24: 1385–1389. https://doi.org/10.7863/jum.2005.24.10.1385

72. Pattanayak S, Chatterjee S, Ravikumar R, Nijhawan VS, Sharma V, et al. (2018) Ultrasound evaluation of cervical lymphadenopathy: can it reduce the need of histopathology/cytopathology? Med J Armed Forces India 74: 227–234. https://doi.org/10.1016/j.mjafi.2017.04.005

73. Ying M, Pang BSF (2009) Three-dimensional ultrasound measurement of cervical lymph node volume. Br J Radiol 82: 617–625. https://doi.org/10.1259/bjr/17611956

74. Gor DM, Langer JE, Loevner LA (2006) Imaging of cervical lymph nodes in head and neck cancer: the basics. Radiol Clin North Am 44: 101–110. https://doi.org/10.1016/j.rcl.2005.08.006

75. Landry CS, Grubbs EG, Busaidy NL, Monroe BJ, Staerkel GA, et al. (2011) Cystic lymph nodes in the lateral neck as indicators of metastatic papillary thyroid cancer. Endocr Pract 17: 240–244. https://doi.org/10.4158/ep10134.or

76. Patil S, Murugalyan SR, Bhaskar P, Ashok D, Aboobaker M, et al. (2021) A vivid way of differentiating benign and malignant cervical lymph node through b-mode ultrasonography and sonoelastography. J Med Allied Sci 11: 172–177. https://doi.org/10.5455/jmas.63227

77. Moharram MA, Abd-ElMaboud NM, Ahmed HA (2017) Evaluation of the role of sono-elastography in diagnosis of enlarged cervical lymph nodes. Egypt J Radiol Nucl Med 48: 381–391. https://doi.org/10.1016/j.ejrnm.2017.01.009